

Article

Effect of Fractionation Columns on the Elution of Rare Earth Elements Recovered from Acid Mine Drainage

Gabriela Cordeiro Silva *, Clauson Souza, Pedro Augusto Possa Vicente Sacramento Ferreira, Liliani Pacheco Tavares Nazareth and Ana Claudia Queiroz Ladeira *

Center for Development of Nuclear Technology, Campus of the Federal University of Minas Gerais, UFMG, CDTN—Av. Antônio Carlos 6627, Belo Horizonte CEP 31270-901, Minas Gerais, Brazil

* Correspondence: gcs2010@ufmg.br (G.C.S.); acql@cdtn.br (A.C.Q.L.)

Abstract: Rare earth elements (REE) can be found in expressive contents in different secondary sources, such as acid mine drainage (AMD). This work evaluated separation of light and heavy rare earth elements (REE) from an acid mine drainage (AMD) generated in a former uranium mine in Brazil by using ion exchange. This AMD presents pH 3.50, total REE content of 97 mg L⁻¹ and 1.3 g L⁻¹ of sulfate and was used in the REE loading experiments. Loading experiments were carried out in columns using a commercial strong acid cation (SAC) exchange resin. Elution was performed with 0.01 mol L⁻¹ NH₄EDTA in systems with one, two and three columns. Regarding the loading step, the resin presented a total loading capacity of 0.58 mmol g⁻¹. The resin proved to be more selective for light REE with adsorption efficiency of 78% and 48% for heavy REE. Regarding elution, high efficiencies between 90 and 100% were achieved for REE. The final REE solution is approximately 10 times more concentrated in the liquor related to the acid mine water. Better fractionation results were achieved for the system with three columns. Although the complete separation of the REE into pure elements was not possible, two distinct fractions of heavy and light REE could be obtained, and La was completely separated from the other REE. In order to improve fractionation and separate the REE into individual ones, the concentrated fractions can proceed to subsequent ion exchange systems.



Citation: Silva, G.C.; Souza, C.; Ferreira, P.A.P.V.S.; Nazareth, L.P.T.; Ladeira, A.C.Q. Effect of Fractionation Columns on the Elution of Rare Earth Elements Recovered from Acid Mine Drainage. *Minerals* **2024**, *14*, 451. <https://doi.org/10.3390/min14050451>

Academic Editors: Ilhwan Park, Patrícia Gomes, Teresa Valente and Juan Antelo

Received: 22 March 2024
Revised: 19 April 2024
Accepted: 23 April 2024
Published: 25 April 2024



Copyright: © 2024 by the authors. Licensee MDPI, Basel, Switzerland. This article is an open access article distributed under the terms and conditions of the Creative Commons Attribution (CC BY) license (<https://creativecommons.org/licenses/by/4.0/>).

Keywords: REE; AMD; ion exchange resin; EDTA; fractionation

1. Introduction

Rare earth elements (REE) are essential raw materials for contemporary technological advancement [1–4]. Due to the volatility and high cost of REE production, there is a growing tendency to explore secondary sources of these elements, such as acid mine drainage (AMD) and the wastes generated by its treatment [4–9]. The large volumes of waste generated, and the high cost associated with treatment turns AMD into one of the greatest mining sustainability challenges. Developing research initiatives to identify the potential benefit of considering AMD as a potential secondary source should be encouraged by new regulatory initiatives on sustainable development as well as the circular economy [9–11].

The treatment of AMD generally comprises the precipitation of metal ions as hydroxides. Nevertheless, this strategy consumes large amounts of alkaline agents, and produces a water-rich sludge, which makes the process expensive [12–15]. For example, the AMD used in this work is generated and treated at a former uranium mine in Brazil through neutralization, and the produced sludge is disposed of in tailing dams. Annually, a total volume of 2.1×10^6 m³ of AMD is treated, consuming 2.9 t of hydrated lime (average consumption of order of 200 t/month) and 1.5 t of flocculant (polyelectrolyte). The monthly cost of treatment, considering only the consumption of these two inputs, varies between R\$800,000.00 and R\$900,000.00 [14].

The concentration/fractionation of REE from dilute solutions such as AMD can be carried out by solvent extraction and/or ion exchange [12,13]. The main drawback with

solvent extraction is the intense use of chemicals, which is reduced by using ion exchange technology [12,13,16]. Ion exchange is a potential key technology to develop more sustainable processes for AMD management compared to traditional treatments [16–18]. Ion exchange resins offer several advantages, including commercial availability, acceptable selectivity, robust mechanical strength, and chemical stability. They effectively recover REE from highly diluted solutions like AMD. Despite these benefits, a dependable process for concentrating and fractionating REE from AMD remains undeveloped. Although advancements in AMD treatment are underway, there remains a scarcity of methods capable of pre-concentrating/fractionating REE from AMD in an environmentally sustainable, cost-effective, and scalable manner [6,7].

The most challenging step in REE production is the fractionation into pure elements, as it entails separating elements with closely similar properties. Few works in the literature deal with using ion exchange to recover REE from AMD and focus on concentrating REE, not fractionating them [6,7,19,20]. Table 1 summarizes previous studies regarding the use of ion exchange technique to recover REE from different aqueous solutions. The first work of our research group showed that ion exchange using cationic resins was promising with 97% recovery of REE from AMD [19]. However, elution with inorganic acids was not effective in terms of both recovery and fractionation, which showed the need for further studies. In addition, another elution study carried out with cationic resins and using different inorganic eluents (acids and salts) showed that calcium chloride presents the highest elution percentages, managing to elute 100% of light REE and almost 90% of heavy REE adsorbed [20]. However, there was no fractionation.

Ethylenediaminetetraacetic acid (EDTA) possesses the advantage of forming highly stable complexes with REE, with the degree of complexation increasing as the atomic number of the elements rises. Consequently, EDTA exhibits a strong affinity for REE, serving as both a complexing agent and an eluting anion, effectively capturing and releasing them from the resin. This robust binding affinity ensures efficient separation and elution of REE, facilitating the process of fractionation. A few studies in the literature have used EDTA as eluent to enhance fractionation [21–25]. These studies primarily concentrate on the pre-concentration of REE in nitric or hydrochloric mediums, despite the prevalence of sulfate medium in industrial production. Unlike chloride and nitrate, sulfate forms stable complexes with REE, resulting in distinct behaviors during loading and elution [20].

Table 1. Summary of works regarding the use of ion exchange to recover REE from different aqueous solutions.

Reference	Loading Conditions	Elution Conditions	Results
[6]	Batch and column experiments; chelating and solvent impregnated resins; AMD from a mine in Spain.	Batch and column experiments with H ₂ SO ₄ as eluent.	Easy separation of REE from transition elements (TEs). The REE concentration factors could reach values up to 20–30.
[7]	Column experiments; SAC resin (Na ⁺ as counter ion); AMD from a mine in Spain.	Column experiments with 1.0 mol L ⁻¹ H ₂ SO ₄ as eluent.	Concentrated REE sulfuric solutions up to 0.25 g L ⁻¹ .
[19]	Batch experiments; commercial SAC resins (Na ⁺ and H ⁺ as counter ions); pH values 1.4, 2.4 and 3.4; sulfate-rich AMD from a closed mine in Brazil.		All resins showed higher loading for La (approx. 0.20 mmol g ⁻¹) and more selective for light REE at all pHs. pHs 1.4 and 3.4 were ideal for the recovery of REE; 97% of REE could be recovered from AMD.

Table 1. Cont.

Reference	Loading Conditions	Elution Conditions	Results
[20]	Batch and column (only for AMD) experiments; commercial SAC resin (H^+ as counter ion); pH values between 3.0 and 4.0; sulfate-rich AMD from a closed mine in Brazil and synthetic La and Y sulfate solutions.	Batch experiments with different eluents ($2.0 \text{ mol L}^{-1} H_2SO_4$, $2.0 \text{ mol L}^{-1} HCl$, $4.0 \text{ mol L}^{-1} NaCl$, $2.0 \text{ mol L}^{-1} CaCl_2$) and column experiments with $2.0 \text{ mol L}^{-1} CaCl_2$.	$CaCl_2$ presented the highest elution percentages, managing to elute 100% of light REE and almost 90% of heavy REE adsorbed. There was no fractionation.
[22,23]	Column experiments; SAC resin (H^+ as counter ion); synthetic heavy REE chloride solutions (between 5 and 6 g L^{-1}).	Column experiments with NH_4EDTA at pH 8.4 as eluent; one fractionation column consisting of two segments of iminodiacetic resin in NH_4^+ and H^+ form; Er as retaining ion.	Over 80% of the heavy REE eluted from the column was separated into fractions with 99% purity of each element.
[24]	Column experiments; SAC resin (H^+ as counter ion); synthetic REE chloride solutions.	Column experiments with $0.015 \text{ mol L}^{-1} NH_4EDTA$ at pH 8.0 as eluent; one fractionation column consisting of SAC resin in H^+ form (H^+ as retaining ion) maintained at temperature from 90 to $120 \text{ }^\circ\text{C}$ to avoid EDTA precipitation.	The REE form individual bands in the second column, resulting in a very effective separation of the REE into the individual species.
[25]	Column experiments; cation exchange resin (Cu as retaining ion); Synthetic Pr, Nd and Dy nitrate solutions.	Column experiments with $0.09 \text{ mol L}^{-1} Na_2EDTA$ at pH 9.0 as eluent; two chromatography columns; Cu as retaining ion.	High-purity (>99%) Pr, Nd and Dy.
[26]	Column experiments; SAC resin (H^+ as counter ion); pH value 3.5; synthetic REE and Al, Ca, Mg sulfate solutions.	Column experiments with 0.3, 0.05 and $0.02 \text{ mol L}^{-1} NH_4EDTA$ at pH 8.56 as eluent. No fractionation columns.	A loading efficiency of 85% for REE and 30% for impurities was achieved. The elution using $0.02 \text{ mol L}^{-1} NH_4EDTA$ promotes the separation of Al and Ca from REE.
[27]	Column experiments; chelating resins (H^+ and Na^+ as counter ions); pH value 3.5; synthetic REE and Al, Ca, Mg sulfate solutions.	Column experiments with 0.05 M NH_4EDTA as eluent. No fractionation columns.	The efficiency of the resins in loading the REE varied from 38% to 73%. Mg could be separated from the REE, and the Ca and Al content in the final liquor was significantly low.
[28]	Column experiments; commercial SAC resin (H^+ as counter ions); pH value 3.5; sulfate-rich AMD from a closed mine in Brazil.	Column experiments with 0.02 and $0.01 \text{ mol L}^{-1} NH_4EDTA$ at pH 8.5 as eluent. One fractionation column consisting of SAC resin in H^+ form (H^+ and NH_4^+ as retaining ion).	Loading efficiencies of 78% for REE and 48% for impurities. The best elution profiles were promoted by $0.01 \text{ mol L}^{-1} NH_4EDTA$. Partial fractionation of REE.

Our recent studies have investigated the use of NH_4EDTA in different concentrations and flow rates as an eluent of REE recovered from a sulfate-rich AMD in order to fractionate them [26–28]. The process of fractionation was greatly enhanced by the use of NH_4EDTA in low concentration, i.e., 0.01 mol L^{-1} along with an additional fractionation column activated with NH_4^+ . It is believed that by combining the best experimental conditions with elution in two or more fractionation columns connected in series, a more pronounced fractionation of the REE can be obtained. Therefore, the present work aims to investigate the effect of the number of fractionation columns, previously activated with NH_4^+ , on the separation of REE recovered from AMD by ion exchange using NH_4EDTA in the elution experiments. The first column, previously saturated with REE, acts as a simple ion concentrator, while the subsequent columns, without REE and previously activated with NH_4^+ , plays a fractionating role. A genuine and complex AMD sample containing

diluted REE in a sulfate medium, most of them essential for the green industry, was used in the experiments. This study can arouse proposals of a more environmentally friendly and efficient method for REE production by ion exchange and secondary sources.

2. Materials and Methods

2.1. Acid Effluent

The acid effluent is generated in the mine pit and in two waste rock piles of a former uranium mine that belongs to a company (*Indústrias Nucleares Brasileiras—INB*) situated in Caldas Municipality (MG-Brazil) [29,30]. The chemical characterization of the acid effluent sample is presented in Table 2.

Table 2. Chemical characterization of the acid effluent sample (pH = 3.5 ± 0.2).

Elements	mg L ⁻¹	mmol L ⁻¹
La	42 ± 2	0.30 ± 0.02
Ce	31 ± 2	0.22 ± 0.01
Pr	3.52 ± 0.2	0.025 ± 0.001
Nd	12.4 ± 0.6	0.086 ± 0.004
Sm	1.45 ± 0.07	0.0096 ± 0.0005
Light REE	90 ± 4	0.64 ± 0.03
Gd	0.74 ± 0.04	0.0047 ± 0.0002
Dy	1.10 ± 0.06	0.0068 ± 0.0003
Y	4.8 ± 0.2	0.053 ± 0.003
Heavy REE	6.6 ± 0.3	0.06453 ± 0.003
Total REE	97 ± 1	0.70 ± 0.04
Total impurities (Al, Ca, Mg, Mn, Fe)	411 ± 21	11.5 ± 0.6
SO ₄ ²⁻	1326 ± 66	13.8 ± 0.7

2.2. Eluent Solution

The 0.01 mol L⁻¹ NH₄EDTA, used as eluent, was obtained by dissolving crystalline EDTA in concentrated ammonium hydroxide (NH₄OH), under heating at 150 °C and permanent stirring. Afterwards, the solution was transferred to a volumetric flask of 2 L, and MILLI-Q deionized water was added and pH adjusted to 8.5.

2.3. Ion Exchange Resin

The resin used for this study was supplied by LANXESS. It is a strong acid resin with an ion exchange functional group -SO₃H (sulfonic acid) and a styrenic matrix. This resin was selected according to previous works [19,20,26–28], producer guidance and commercial availability. Before using it, it was washed with MILLI-Q deionized water. Resin properties are summarized in Table 3.

Table 3. General properties of the resin.

Name	LEWATIT® MDS 200H
Type	Strongly acidic cation
Functional group	Sulfonic (SO ₃ H ⁻)
Ionic form	H ⁺
Matrix	Styrenic
Size (mm)	0.33 ± 0.05
Water retention (%)	45–50
Operation pH	0–14
Volume variation	8%
Ion exchange capacity (eq L ⁻¹)	2.3
Density (g mL ⁻¹)	1.2

The activation of the resin with NH_4^+ consisted of passing a 10% NH_4OH solution through columns with 15.5 ± 0.5 mL of resin bed, at a constant flow rate of 3 BV h^{-1} until the outlet pH was equal to the inlet pH. Soon after, the passage of deionized water began at the same previous flow rate until the effluent outlet pH was close to neutral.

2.4. REE Loading Experiments

The loading experiments were conducted in triplicate using a glass column with an internal diameter of 11 mm. The mass of the resin for the loading experiments was 6.25 g of Lewatit MDS 200H resin (dry basis). After adding the resin to the column vessel, the resin bed was washed with deionized water. The AMD solution (Table 2) was percolated through the column by peristaltic pumps (Qdos 30, Watson-Marlow Limited, Falmouth, UK) in a downward flow at a constant temperature of $25 \text{ }^\circ\text{C}$ and a constant flow rate of $0.78 \pm 0.01 \text{ mL min}^{-1}$, which corresponds to a residence time of 10.2 min. The effluent leaving the column was led through a polyethylene hose to a fractionating sampler (Frac-900, Amersham Pharmacia Biotech Limited, Uppsala, Sweden) and samples were collected for REE analysis. After completing the loading of REE, the bed was washed with deionized water, and the water level in the bed was maintained approximately 3.0 cm above the resin level until the elution tests were carried out.

The amount of each REE adsorbed by the resin during loading (Q) can be determined by the breakthrough curve [18]. Considering the inlet concentration of each metal as C_0 , and the outlet concentration as C , the amount of metal Q adsorbed per gram of resin is defined by Equation (1) and calculated by using OriginPro 2024 software (10.1.0.170 Learning Edition, OriginLab Corporation, Northampton, MA, USA).

$$Q = \int_{BV_1}^{BV_2} (C_0 - C) dBV \quad (1)$$

where Q is the adsorbed amount of metal on the resin in mmol g^{-1} ; V_{BV} is the bed volume in L; M_{BV} is the mass of resin on a dry basis of the bed in g; BV_1 is the effluent input volume in BV; BV_2 is the effluent output volume in BV; C_0 is the feed concentration of each metal in mmol L^{-1} ; and C is the column outlet concentration in mmol L^{-1} . Loading efficiency (E_f) is calculated from Equation (2).

$$E_f = (m_q/m_{\text{feed}}) \times 100\% \quad (2)$$

where m_q is the REE mass loaded in the resin and m_{feed} is the REE mass in the feed solution.

2.5. REE Elution Experiments

Elution tests were carried out in duplicate with more than one column to study the effect of the number of columns on fractionation. The columns were connected in series. The first one with 8.0 ± 0.5 mL of bed was previously saturated with REE and the others with 15.5 ± 0.5 mL of bed were activated with NH_4^+ [28]. The interconnected systems with one, two and three columns in series were eluted under the pre-determined experimental conditions such as: NH_4EDTA solution at 0.01 mol L^{-1} at pH 8.5, $25 \pm 5 \text{ }^\circ\text{C}$, residence time of 23 ± 1 min and flow rate of $0.35 \pm 0.02 \text{ mL min}^{-1}$. NH_4EDTA was introduced at the top of the column saturated with REE, and then continues to the top of the second column, and so on, using peristaltic pumps. The column effluent was collected using an automatic fraction collector every 45 min. Figure 1 presents a schematic design for the experimental apparatus used in this study.

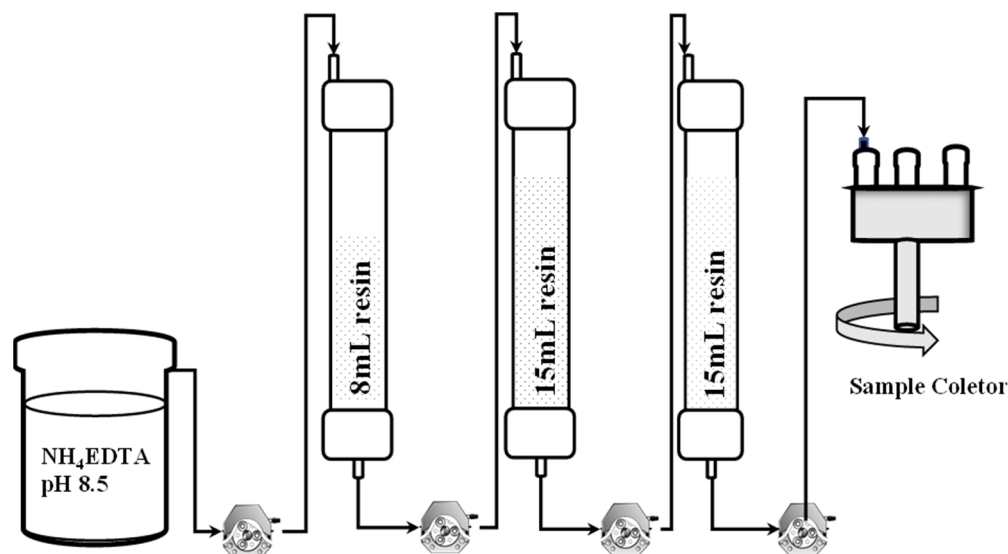


Figure 1. Experimental apparatus used in the resin elution tests with one saturated column (8 mL) and two fractionating columns (15.5 mL) activated with NH_4^+ .

2.6. Chemical Analyses

The concentrations of REE in the liquid samples were determined using the inductively coupled plasma optical emission spectrometry technique (ICP OES; SPECTRO/SPECTRO ARCOS), with axial configuration, crossflow nebulizer and wavelength range of 130 (160)—770 nm. Using a multi-element standard solution, the calibration curve was constructed, obtaining a linear range as a response for each element. Precision and accuracy were also adequate at the concentration levels studied, with the standard deviation being less than 3% and the limits of quantification (LOQ) of this method being 0.10 mg L^{-1} for REE.

3. Results and Discussion

3.1. REE Loading

Table 4 presents the loading values Q (mmol g^{-1}) and the percentage of REE removed from the feed solution after percolation of 800 BV of the AMD (in Table 2). The percentage of light REE (LREE) (La, Ce, Pr, Nd and Sm) removed was 80%. Individually, LREE removal varied from 64% for Sm to 88% for La. Regarding heavy REE (HREE) (Gd, Dy and Y), their removal was 40%, varying individually between 38% for Y and 51% for Gd. The total REE adsorbed by the resin was $0.580 \text{ mmol g}^{-1}$ of which $0.549 \text{ mmol g}^{-1}$ was made up of LREE and $0.031 \text{ mmol g}^{-1}$ of HREE. Studies assessing various ion-exchange resins for the selective recovery of REE from acid mine waters have consistently highlighted the superior selectivity of sulfonic resins for LREE over HREE, resulting in optimal selectivity factors for REE extraction [6,7,19].

Table 4. Loading Q (mmol g^{-1}) of the REE by the resin Lewatit MDS 200H (Lanxess, Cologne, Germany) and the percentage of REE removed from the feed solution.

Elements	La	Ce	Pr	Nd	Sm	Gd	Dy	Y	LREE	HREE	REE
Q (mmol g^{-1})	0.282	0.186	0.017	0.058	0.006	0.003	0.003	0.025	0.549	0.031	0.580
% REE Removed	88.0	77.0	69.0	64.0	74.0	51.0	61.0	38.0	80.0	40.0	70.0

The Lewatit resin showed greater affinity towards LREE than for HREE, which is in line with previous studies that use the same adsorbent to recover REE from AMD effluent [19,20,26,28]. These studies, in addition to showing the greater affinity of the resin

for the LREE, also demonstrate that there is a displacement of part of the HREE adsorbed on the resin by the LREE, mainly La, as it is the most electropositive REE (with a greater basic character), with a higher content in feed solutions. A previous work [27] demonstrated that during the loading of REE, desorption of elements, such as Nd, Sm, Dy, Gd and Y also occurs. As a consequence, La presented curves with an elongated profile (a long-tail profile), contrary to the other REE (Nd, Sm, Gd, Dy and Y) which presented profiles with a more abrupt growth. The lengthening of the curves occurs because as the heavier REE are desorbed, the lighter elements La, Pr and Nd occupy the released sites. La is the element that most replaced the desorbed elements and, therefore, presents the most elongated profile. Y presents greater desorption and the sharpest peak.

Figure 2 shows REE distribution in the feed solution and in the resin after loading through the molar ratios of each REE present over the total REE (REE/TREE). It is observed that the molar ratio of LREE/TREE increased from 90.9% in the AMD to 94.7% in the resin. As a result, the HREE/TREE molar ratio decreased from 9.1% in the feed to 5.3% in the resin. As we see in Table 4, La showed the highest adsorption ($0.282 \text{ mmol g}^{-1}$), and consequently, the La/TREE molar ratio increased from 42.5% in the AMD to 48.6% in the resin. For the other LREE (Ce, Pr, Nd and Sm), there was no considerable change in the molar composition of these elements in the resin in relation to the feed. Regarding HREE adsorption, Y presented the highest adsorbed amount ($0.025 \text{ mmol g}^{-1}$). In turn, Gd and Dy presented similar adsorbed amounts ($0.003 \text{ mmol g}^{-1}$) maintaining similar REE/TREE molar ratios both in the feed ($\sim 1\%$) and in the resin (0.5%). The molar ratio Y/REE decreased from 7.5% in the feed to 4.3% in the resin.

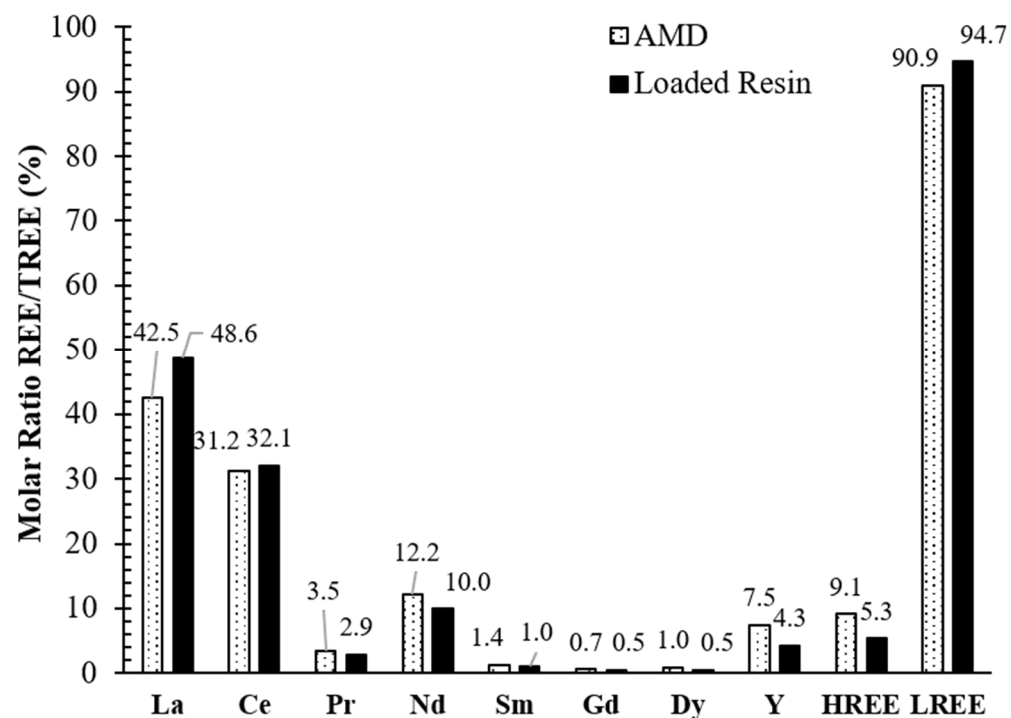
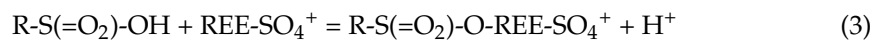


Figure 2. REE distribution in the feed solution and in the resin after loading. AMD—acid mine drainage (Table 2); loaded resin (Table 4).

The REE loading of the ion exchange resin occurs when the resin's counter ion is released (displaced) by the ionic species present in the solution according to their affinity with the resin. In the sulfate-rich acid effluent, the SO_4^{2-} ions can complex REE and Al through one or two coordinated bonds. The formation of such complexes directly influences the REE's demand for active sites on the resin. In the physical-chemical conditions in which the acidic effluent is present ($[\text{REE}]_{\text{Total}} = 0.70 \text{ mmol L}^{-1}$, $[\text{SO}_4^{2-}] = 13.8 \text{ mmol L}^{-1}$ and $\text{pH} = 3.5 \pm 0.2$), REE are primarily in the form REE-SO_4^+ [31]. A previous work [20],

through electronic structure calculations using density functional theory (DFT), presents a model for the adsorption of REE sulfate complexes on the ion exchange resin. The calculations simulate the interactions of the functional group of the cationic resin -RSO_3^+ with the sulfated species and sulfate-free ions of La and Y, and considered the following species: REE^{3+} , REE-SO_4^+ e $\text{REE-(SO}_4)_2^-$. The free energy data show that the interaction between the functional group and the REE-SO_4^+ species that presented the lowest energy and, therefore, should be the REE species preferentially adsorbed by the cationic resin (Equation (3)).



A couple of works in the literature compile the values for the formation constants of the REE-SO_4^+ and $\text{REE(SO}_4)_2^-$ complexes (La, Ce, Pr, Sm, Nd, Gd, Dy and Y) [31,32]. The formation constants are very close to each other, which should correspond to very similar behaviors in the adsorption of all REE. In Equation (4), the REE-SO_4^+ formation reaction is presented, with the values of the formation constants being in the range of $3.4 \leq \log\beta \leq 3.8$.



3.2. REE Elution from the Loaded Resin Column

Figure 3 shows the elution of REE by a solution of 0.01 mmol L^{-1} NH_4EDTA from a Lewatit MDS200H resin column loaded with the acid effluent from Table 2.

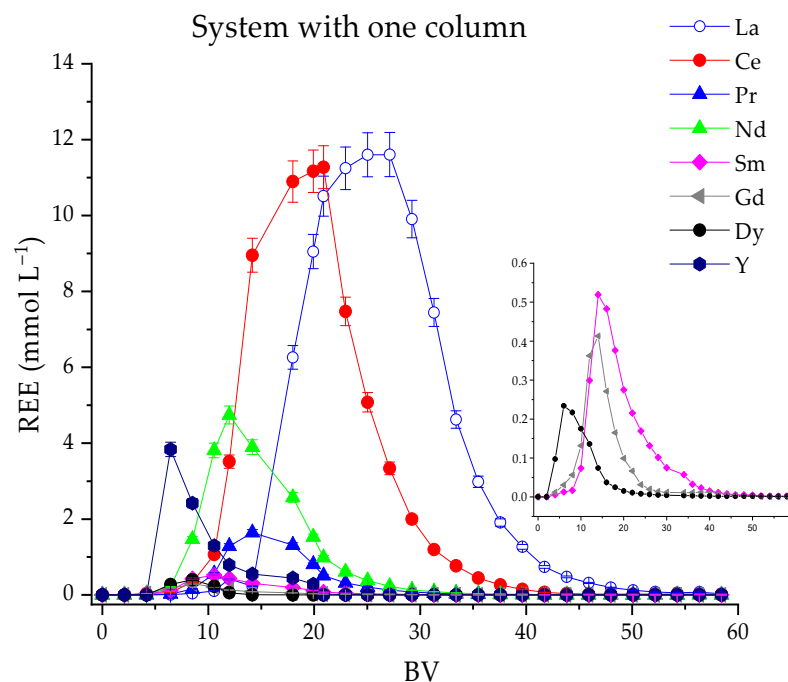


Figure 3. Evolution of the recovery and composition of the eluate as a function of the BV fraction collected in the elution of the 8.0 mL Lewatit MDS 200H resin saturated with REE; $[\text{NH}_4\text{EDTA}] = 0.01 \text{ mol L}^{-1}$; $\text{pH}_{\text{initial}} = 8.5$; temperature: $25 \pm 5 \text{ }^\circ\text{C}$; and flow rate: $0.35 \pm 0.02 \text{ mL min}^{-1}$.

It is possible to observe that the peaks of the highest concentrations for Pr, Nd, Sm, Gd, Dy and Y occur relatively close and below 14 BV, indicating that there is no significant fractionation for these REE. However, it is noticeable that at the beginning of the elution, there is a preferential elution of HREE. Up to 6 BV, the composition of the accumulated volume is 77% HREE and 23% LREE. However, at this point, HREE recovery is only 19%. Up to 10.4 BV, the composition of the accumulated volume is 41.9% of HREE and 58.1% of LREE, but the recovery of LREE is only 7%, while for HREE it rises to 82%. From

25 BV onwards, La and Ce are eluted practically isolated from the rest of the other REE, signaling important fractionation. A study from the literature investigated the elution of a sulfonic resin pre-saturated with REE from AMD using $1.0 \text{ mol L}^{-1} \text{ H}_2\text{SO}_4$, demonstrating a significant increase in REE concentration factors of up to 260. However, no fractionation was observed [7]. In addition, our previous research, which utilized EDTA as an eluent for REE-saturated resins, revealed that the elements were eluted in close bed volumes (BVs), with superimposed bands and low percentages in the elution peaks, indicating poor fractionation [26–28].

3.3. pH Evolution and REE Species during Elution

It is well established that REE^{3+} ions in aqueous solution form stable complexes (1:1) with the chelating agent EDTA [33]. The complexation equilibrium between EDTA and REE^{3+} is given by:



where K_F is the equilibrium constant described as $[\text{REE-EDTA}^-]/([\text{REE}^{3+}][\text{EDTA}^{4-}]$.

In the literature, the preference for elution of HREE over LREE is attributed to the high formation constants (K_F) of HREE-EDTA⁻ complexes relative to LREE-EDTA⁻ complexes [31–35]. Since H_4EDTA is a weak polyprotic acid, it dissociates into mono-, di-, tri- and tetra-neutralized as a function of the pH of the aqueous system ($\text{p}K_{a1} = 2.0$; $\text{p}K_{a2} = 2.6$; $\text{p}K_{a3} = 6.0$; $\text{p}K_{a4} = 10.2$) and the concentration of the total EDTA is described by Equation (6).

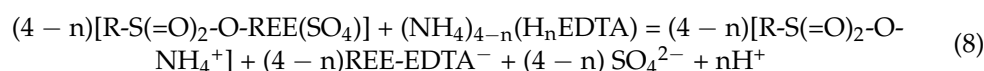
$$[\text{EDTA}]_{\text{Total}} = [\text{H}_4\text{EDTA}] + [\text{H}_3\text{EDTA}^-] + [\text{H}_2\text{EDTA}^{2-}] + [\text{HEDTA}^{3-}] + [\text{EDTA}^{4-}] \quad (6)$$

Under the experimental conditions of the present work, i.e., $[\text{NH}_4\text{EDTA}] = 0.01 \text{ mol L}^{-1}$ and initial pH 8.5, EDTA is predominant in the form HEDTA^{3-} . However, previous studies on REE elution have demonstrated that during eluent percolation, there is a decrease in the pH [21–26]. Considering that the amount of EDTA^{4-} required for REE^{3+} complexation is pH dependent, it is possible to determine the α fraction of EDTA^{4-} , i.e., $\alpha_{\text{EDTA}^{4-}} = [\text{EDTA}^{4-}]/[\text{EDTA}]_{\text{Total}}$ as a function of pH using Equation (7) [23,26].

$$\alpha_{\text{EDTA}^{4-}} = (K_{a1} \cdot K_{a2} \cdot K_{a3} \cdot K_{a4}) / \text{DELTA} \quad (7)$$

where $\text{DELTA} = [\text{H}^+]^4 + K_{a1} \cdot [\text{H}^+]^3 + K_{a1} \cdot K_{a2} \cdot [\text{H}^+]^2 + K_{a1} \cdot K_{a2} \cdot K_{a3} \cdot [\text{H}^+] + K_{a1} \cdot K_{a2} \cdot K_{a3} \cdot K_{a4}$

It is important to consider that the REE can also be present in the REE-SO_4^+ form and the interactions of REE^{3+} with the complexants present in the aqueous medium must be evaluated [20]. The formation constants for the complexation of REE adsorbed on the resin, whether in the REE^{3+} form or in the REE-SO_4^+ form are presented in Table 5. Such interactions will be considered here through the values of the constant $\beta_{\text{REE-SO}_4^+}$. The overall elution reaction of the REE-SO_4^+ complex by NH_4EDTA occurs according to Equation (8) [20].



where $\text{R-S(=O)}_2\text{-O}$ is the sulfonic functional group of a strongly acidic resin, and n is the number of protons present in EDTA according to the pH of the medium. With this, the global formation constants K_{FSO_4}' have their values defined as shown in Equation (9).

$$K_{\text{FSO}_4}' = K_F \beta_{\text{EDTA}^{4-}} \beta_{\text{REE-SO}_4} \quad (9)$$

Table 5. REE formation constants for the systems REE-EDTA and REE-SO₄-EDTA in aqueous medium.

Elements	Formation Constant K _F [34]	β _{REE-SO₄⁺} [20,31,35]	Formation Constant K _{F_{SO₄'}}
La	2.19 × 10 ¹⁶	4.17 × 10 ³	5.25 × 10 ¹²
Ce	6.31 × 10 ¹⁶	2.51 × 10 ³	2.51 × 10 ¹³
Pr	3.55 × 10 ¹⁶	4.17 × 10 ³	8.51 × 10 ¹²
Nd	3.98 × 10 ¹⁶	4.47 × 10 ³	8.91 × 10 ¹²
Sm	2.69 × 10 ¹⁶	3.39 × 10 ³	7.94 × 10 ¹²
Gd	1.58 × 10 ¹⁷	4.57 × 10 ³	3.47 × 10 ¹³
Dy	1.00 × 10 ¹⁸	6.76 × 10 ³	1.48 × 10 ¹⁴
Y	2.09 × 10 ¹⁸	2.51 × 10 ³	8.32 × 10 ¹⁴

$$K_F = \frac{[REE-EDTA^-]}{([REE^{3+}][EDTA^{4-}])}$$

$$\beta_{REE-SO_4^+} = \frac{[REE-SO_4^+]}{([REE^{3+}][SO_4^{2-}])}$$

$$K_{F_{SO_4}'} = \frac{[REE-EDTA^-]}{([REE^{3+}][EDTA^{4-}][SO_4^{2-}])}$$

When analyzing Equations (6) to (9) together, it is possible to infer that the elution reaction will cause a drop in the pH of the NH₄EDTA solution, consequently, a decrease in the K_{F_{SO₄'} formation constants and, therefore, a reduction in the probability of such a reaction. Therefore, according to Table 5, the conditional formation constant K_{F'} = αEDTA⁴⁻ · K_F will be smaller than the constant K_F. This effect can be proven through the data presented in Figure 4, where the evolution of pH is shown according to the volume of eluate percolated through the column.}

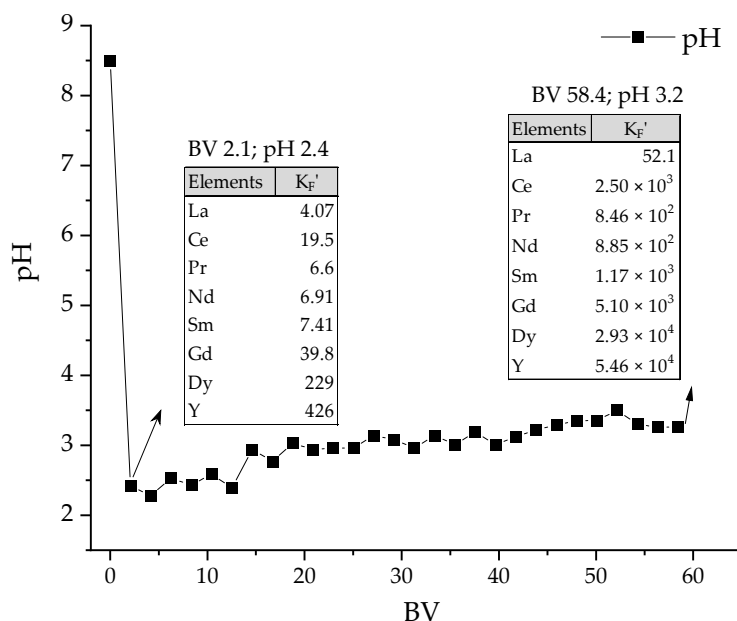


Figure 4. Evolution of outlet pH according to the volume of eluate (BV). Bed volume: 8 mL, Lewatit MDS 200H resin saturated with REE; [NH₄EDTA] = 0.01 mol L⁻¹; initial pH: 8.5; temperature: 25 ± 5 °C; and flow rate: 0.35 ± 0.02 mL min⁻¹. The values of the K_{F_{SO₄'} formation constants for REE are presented considering the pH of the first and last BVs.}

As shown in Figure 4, right at the beginning of elution, there is a sudden drop in pH from 8.5 to 2.4, which is maintained up to 12.5 BV. At this point, around 90% of HREE (Gd, Dy and Y) was eluted; however, the total elution of LREE was around 13%. The K_{F_{SO₄'} data shown in Figure 4 reinforce the effect of pH on the formation constants of REE-EDTA⁻ species, and consequently, on the selectivity and quantity of each eluted species. When comparing the elution data from Figure 3 with the pH data from Figure 4, it is seen that the drop in pH values directly impacts the selective elution of HREE in detriment to}

LREE, especially with regard to Ce and La. At pH 2.4, there is an effective decrease in the $\alpha_{\text{EDTA}^{4-}}$ fraction according to Equation (7) which disfavors the complexation of REE or their desorption from Lewatit MDS 200H resin (Equation (8)). This decreases the values of the complexation equilibrium constants $K_{\text{FSO}_4'}$. Therefore, there is a considerable decrease in the spontaneity of the complexation reaction. According to $K_{\text{FSO}_4'}$ data, at pH 2.4, HREE have values ranging between 39.8 (Gd) and 426 (Y). In contrast, the constants $K_{\text{FSO}_4'}$ for LREE vary from 0.426 (La) to 19.5 (Ce), with the values for Nd, Pr and Sm being relatively close to each other. Due to the higher formation constants of the HREE-EDTA complexes, and the decrease in these values with the decrease in the pH of the eluent, it is possible to observe the overlap of the Y elution curve, reaching its maximum concentration of 3.8 mmol L^{-1} at 6.3 BV (Figure 3). After passing 14.6 BV, when there is an increase in the outlet pH from 2.4 to 2.9, the total elution of Y has already exceeded 93%. The Dy concentration peak (0.40 mmol L^{-1}) is also reached at 6.3 BV and, around 12.5 BV, elution reaches its totality. The peak concentration of Gd, $0.029 \text{ mmol L}^{-1}$, is reached at 8.3 BV; however, its elution continues smoothly up to 20 BV.

The elution of LREE begins with Sm at 4 BV (Figure 3), reaching its peak concentration in the eluate ($0.052 \text{ mmol L}^{-1}$) at 10.4 BV, and exceeding 97% recovery at 25 BV. In relation to Nd, its peak concentration (4.74 mmol L^{-1}) is reached at 12.5 BV, corresponding to 60.4% recovery and, after percolation of 20.9 BV, around 97% of the Nd is recovered. Regarding Pr, the elution curve appears wider in relation to other LREE, with the peak concentration at 1.64 mmol L^{-1} and 14.6 BV. Considering the loading values of the Lewatit MDS 200H resin, the loading of Nd, Pr and Sm is $0.081 \text{ mmol g}^{-1}$, while the loading of La and Ce amount to $0.468 \text{ mmol g}^{-1}$. Even with La and Ce that have loading concentrations higher than the other LREE, elution of these metals occurs at a higher BV, generally after the elution of most REE. The Ce and La concentration peaks occur, respectively in the range of 16–21 and 23–27 BV and the outlet pH is close to 3. Therefore, comparing the pH values during the elution of LREE with those of $K_{\text{FSO}_4'}$, it is possible to link the subsequent elution of La to the value of its complexation constant. It is also possible to observe that Ce and La are eluted practically alone after 23 BV, signaling a significant fractionation of this REE. An elution study with NH_4EDTA of a resin loaded with an AMD solution containing a low concentration of Ce ($0.008 \text{ mmol L}^{-1}$) showed that the Ce elution peak occurs after the Sm, Nd and Pr elution peaks [28]. In addition to the effect of pH on the REE-EDTA⁻ formation constants, there is an effect of the lower lanthanide contraction of Ce and La on the selectivity of REE [26]. The basicity of Ce^{3+} and La^{3+} negatively affects the stability of their complexes (La-EDTA⁻ and Ce-EDTA⁻), where a smaller ionic radius leads to the formation of a stronger complex [2,36]. On the other hand, this more basic character of La and Ce favors their affinity for the strongly acidic cation resin, thus making their elution difficult.

3.4. Effect of Adding Fractionation Columns in the REE Elution Profile

Figure 5 shows the effect of adding one or two $15.5 \pm 0.5 \text{ mL}$ fractionation columns, previously activated with NH_4^+ (Figure 1), on the REE concentration profile in the eluate. This effect is evident when observing the changes in the BV values necessary for the eluate to reach the maximum elution values presented in Table 6.

The elution of REE using the systems with two and three columns (Figure 5a,b) needed more than 80 BV to be completed. Moreover, the increase in fractionation columns caused the spreading of the elution bands. However, the fractionation profiles for these systems show a good separation between La and the other REE. This indicates that the retaining ion fulfilled its role of delaying the elution of La, which has less affinity with the eluent. For the system with two columns (Figure 5a), there is a small separation between the heaviest REE (Y and Dy) and the lightest (Pr, Nd and Ce), except Sm and Gd, while in the system with three columns (Figure 5b), this separation increases. The elution percentages of REE are similar for both systems, except for La, Ce, Pr and Nd, that are lower for the system

with three columns as the elution of La has not started at 80 BV and the elution of Ce, Pr and Nd have not finished.

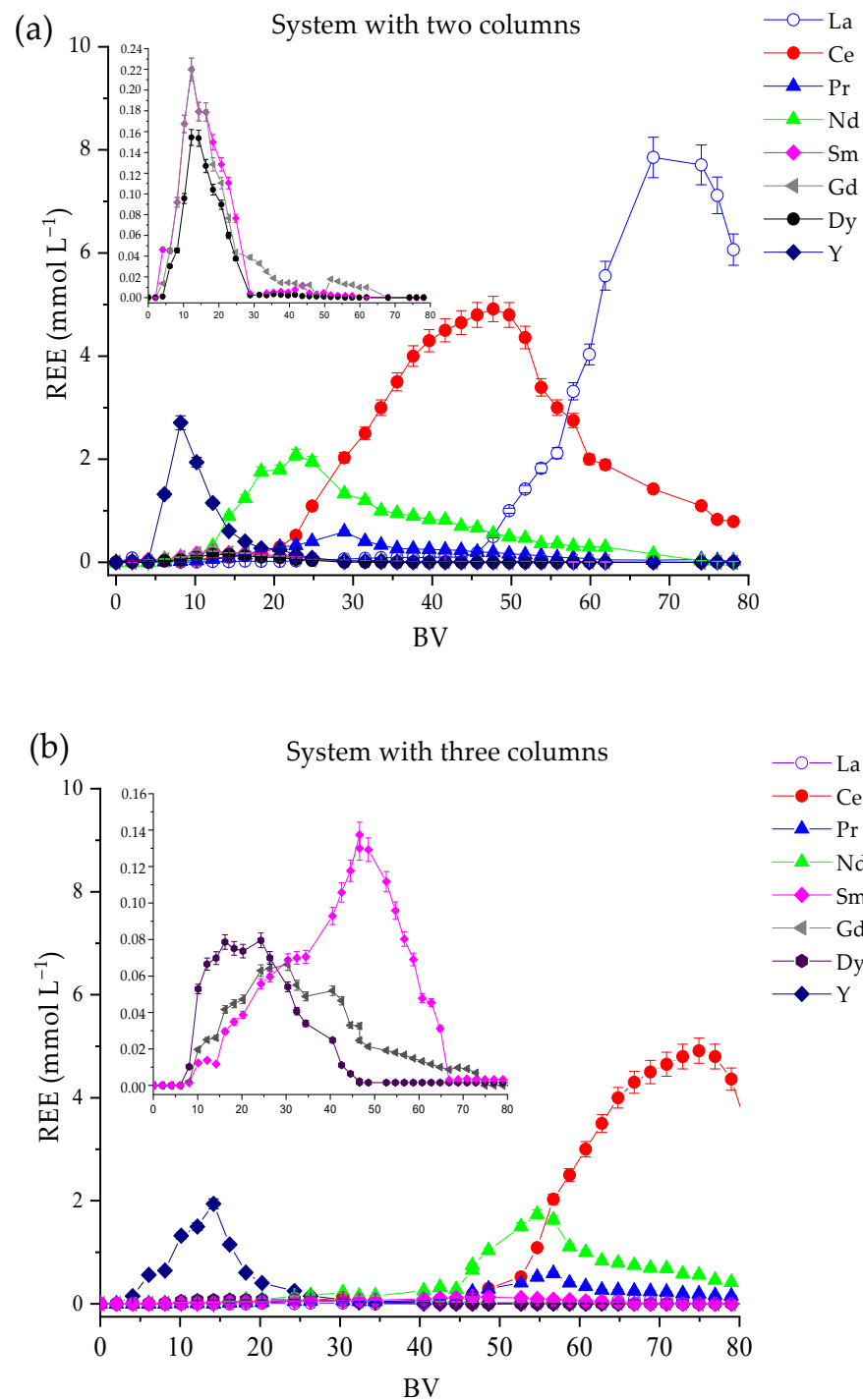


Figure 5. Effect of adding columns on REE fractionation profiles in the elution of Lewatit MDS 200H resin; $[\text{NH}_4\text{EDTA}] = 0.01 \text{ mol L}^{-1}$; temperature: $25 \pm 5 \text{ }^\circ\text{C}$; and flow rate: $0.35 \pm 0.02 \text{ mL min}^{-1}$. (a) Elution in two columns, the first being saturated with REE with BV = 8.0 mL and the second with BV = 15.5 mL, activated with NH_4^+ ; (b) elution in three columns: first one saturated with REE and BV = 8.0 mL; and second and third one activated with NH_4^+ and BV = 15.5 mL.

For the saturated column, the elution is carried out with NH_4EDTA at a pH of 8.5; however, the solution that enters the fractionation column presents a considerably lower pH value as it turns acidic during percolation through the saturated one (Figure 4). The

separation between light and heavy REE can be attributed to the occurrence of several interactions (adsorption/desorption) mainly with the light ones, during the percolation of the eluate in the fractionation column [28]. This factor should be intensified due to the drop in the pH of the eluate.

Table 6. REE concentration values at the elution peak according to the number of fractionation columns. Resin loaded with 0.58 mmol g^{-1} . Elution conditions: flow rate 0.35 mL min^{-1} , initial pH 8.5, $25 \text{ }^\circ\text{C}$ and $0.01 \text{ mol L}^{-1} \text{ NH}_4\text{EDTA}$.

Elution of REE from the Saturated Column								
REE	La	Ce	Pr	Nd	Sm	Gd	Dy	Y
Conc Peak (mmol L^{-1})	11.6	11.3	1.6	4.7	0.5	0.3	0.4	3.8
Peak BV	27.1	20.9	14.6	12.5	10.4	8.3	8.3	6.3
Elution Recovery (%)	86.5	96.0	100.0	100.0	100.0	98.9	100.0	100.0
Elution of REE from saturated column + 1 fractionation column activated with NH_4^+ .								
REE	La	Ce	Pr	Nd	Sm	Gd	Dy	Y
Conc Peak (mmol L^{-1})	7.9	4.9	0.6	2.1	0.2	0.2	0.2	2.7
Peak BV	68.5	47.7	29.0	22.8	14.3	14.3	12.3	8.2
Elution Recovery (%)	83.7	100.0	97.2	100.0	85.2	100.0	93.4	94.9
Elution of REE from saturated column + 2 fractionation columns activated with NH_4^+ .								
REE	La	Ce	Pr	Nd	Sm	Gd	Dy	Y
Conc Peak (mmol L^{-1})	0.1	4.9	0.6	1.7	0.1	0.1	0.1	1.9
Peak BV	73.0	74.9	56.7	54.7	46.6	24–30	16–24	14.2
Elution Recovery (%)	0.9	73.0	90.1	83.3	84.1	91.9	95.1	96.1

As demonstrated in Equation (8), the equilibrium of the REE complexation reaction during elution is unfavorable, favoring adsorption in the form of REE-SO_4^+ . Since the complexation constants (K_F) of LREE-EDTA^- are lower than the constants of HREE-EDTA^- , decomplexation will occur primarily in relation to the anionic species of LREE in LREE^{3+} or LREE-SO_4^+ , followed by re-adsorption of the cationic form by the resin. If such a phenomenon occurs over a period of time, a split between LREE and HREE will certainly occur.

Although the separation of the REE into concentrated fractions of LREE or HREE was feasible in the present study, the separation into pure elements was not attained. High elution efficiencies between 90 and 100% were achieved for REE. Table 6 shows concentrations of REE in fractions for the systems with one saturated column and one or two fractionating columns. These are approximately 10 times more concentrated in the eluate than in the acid mine water, i.e., 0.58 and 5.3 mmol L^{-1} , respectively. For the elution of just one column (Figure 3), it can be seen that it is not necessary to run the experiment up to 80 BV since the elution ends at 30 BV and, consequently, REE will be more concentrated in the final liquor. In order to improve the fractionation and separate the REE into individual ones, the distinct fractions can proceed to a new cycle of loading and elution. The literature reports that higher REE concentrations in the feed solution produces better-defined fractionation profiles with sharper and more separated bands. The attainment of this profile using diluted solutions such as AMD is much more difficult. A couple of works in the literature explored the utilization of a fractionation column divided into two segments, each containing iminodiacetic resin. The first segment employed the resin in NH_4 form, while the second utilized the resin in H^+ form. Erbium served as the retaining ion, and EDTA at pH 8.4 acted as the eluent. This approach enabled the separation of REE into fractions, with each element achieving 99% purity [22,23]. Another work employed interconnected columns activated with copper to separate REE. Their system, incorporating a novel zone-splitting method, comprised two zones: zone I generating two mixed bands that fed into the columns of zone II. Elution was conducted with 0.09 M EDTA at pH 9.0, yielding high-purity (>99%) REE [25]. There is also a patent which has successfully separated REE using a fractionating column equipped with sulfonic acid

type resin in H⁺ form. The eluent, 0.015 M EDTA at pH 8.0, maintained the fractionating column temperature between 90 and 120 °C to prevent EDTA precipitation [24]. Notably, the studies mentioned utilized laboratory solutions with REE concentrations exceeding 5 g L⁻¹, which is significantly higher than those employed in the present study.

With the use of fractionation columns, the eluate from the saturated column will have a longer residence time and, therefore, greater fractionation occurs. According to the experimental conditions, the linear velocity of the eluate in the saturated column is 0.37 cm min⁻¹, meaning that the eluate will take 44.3 min to pass through each fractionation column. In order to illustrate the effect of the interaction between the fractionation column and the REE present in the percolated solution, the amount of REE retained during passage through the fractionation column is given by Equation (10).

$$\%m_{\text{REE}}\text{Retained}(i) = (m_{\text{REE}}\text{Column}_{\text{Loading}}(i) - m_{\text{REE}}\text{Column}_{\text{Fraction}}) \times 100\% / (m_{\text{REE}}\text{Column}_{\text{Loading}}) \quad (10)$$

where %m_{REE}Retained is the mass of REE retained in the fractionation column; (i) is the volume in BV percolated in the set of resin columns; m_{REE}Column_{Loading}(i) is the mass of REE eluted from the loading column in BV(i) fed to the fractionation column; and m_{REE}Column_{Fraction} is the mass of REE in the eluate collected at the outlet of the fractionation column.

Figure 6 shows the mass (%) of REE retained in the fractionation columns after passing through the REE-saturated column. Negative values indicate that REE is released from the fractionation column.

As can be seen in Figure 6a, the retention of HREE during elution occurs mainly in the first 6 BVs for the fractionation columns activated with NH₄⁺. Around 60% of the total HREE (Gd, Dy and Y), contained in the eluate from the saturated column, is retained. Then, after 7 BV the retention of HREE drops drastically to 10% and in the next BVs there is no more HREE retention. Above 60 BV, there is a release of adsorbed REE indicated by negative Mass Retention (%) values. Regarding the LREE, it is observed that there is an increase in retention, reaching 81% in the 19–24 BV fraction. After 35 BV there is a decrease in the LREE retention. From Figure 6b, a greater retention of REE and a more pronounced displacement is seen. Up to 60 BV, there is a retention of 76.6% of LREE, and after 87 BV, 43% is released.

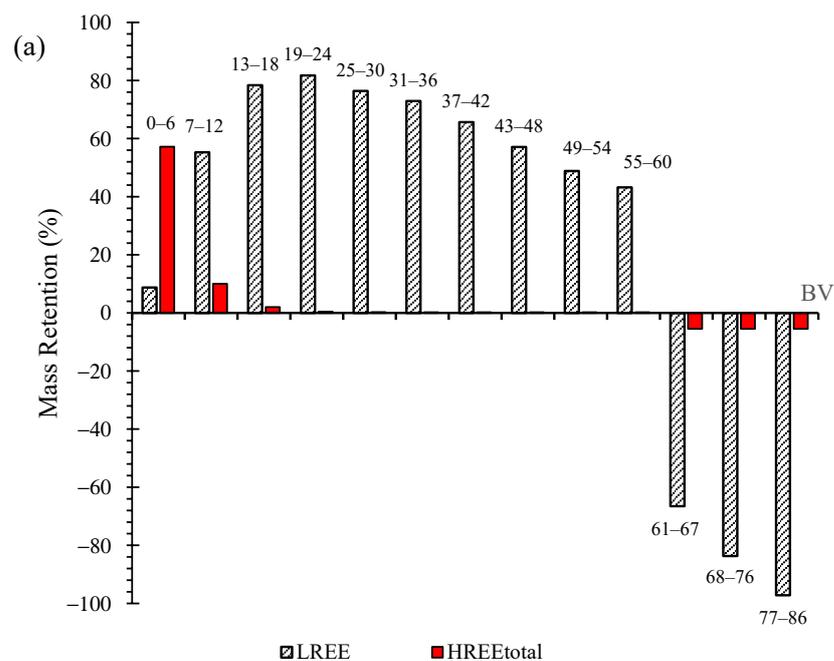


Figure 6. Cont.

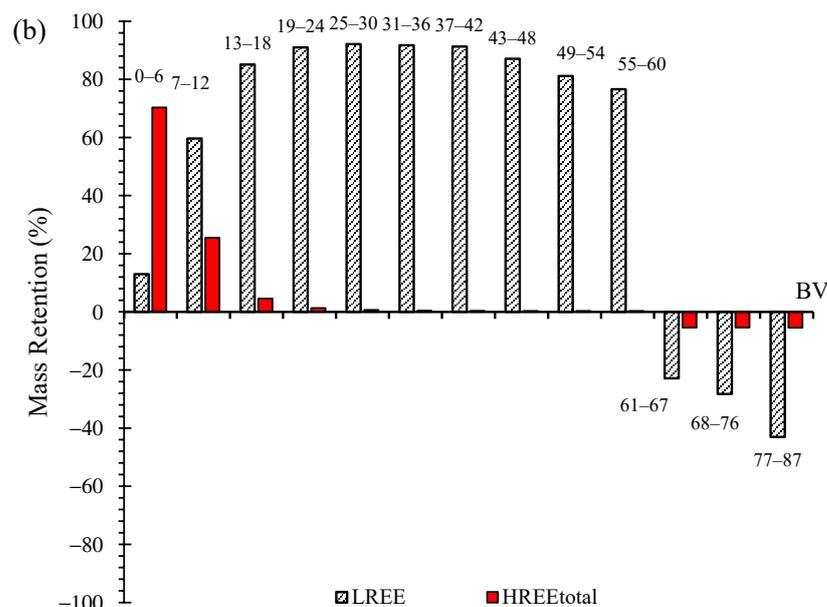


Figure 6. Mass (%) retained in the fractionation columns for (a) one 15.5 mL fractionation column activated with NH_4^+ and (b) two 15.5 mL fractionation columns activated with NH_4^+ .

4. Conclusions

After elution, REE are approximately 10 times more concentrated in the eluate than in the acid mine water, i.e., 0.58 and 5.3 mmol L^{-1} , respectively. The elution of the column, filled with the resin Lewatit MDS 200H saturated with REE, by percolating 0.01 mol L^{-1} NH_4EDTA did not promote a good fractionation between LREE and HREE; only La and Ce were eluted separately. However, the interconnection of this column—saturated with REE—with columns activated with NH_4^+ proved to be efficient in fractionating. The use of one fractionation column allowed a higher concentration of HREE to be achieved, since it retained a more considerable amount of LREE for a longer period. The addition of a second fractionation column provided an additional increase in the LREE retention level. Although the complete separation of the REE into pure elements was not possible, fractions of eluate with elevated concentrations of light or heavy REE could be obtained. Considering the amount of REE absorbed by the Lewatit MDS resin (0.580 mmol g^{-1} of resin is composed of 94.7% LREE and 5.3% HREE), by using two fractionation columns it was possible to obtain one fraction (1 BV to 26 BV) with 88% HREE and 12% LREE on a molar basis. From 27 BV to 87 BV, the fraction was composed of 98.5% LREE and 1.5% LREE on a molar basis. The drop in the eluate pH appears to be the main factor responsible for the preferential elution of HREE since at more acidic pH values, the LREE- EDTA^- complexes present much lower formation constants than LREE- EDTA^- .

The use of an actual effluent, which is complex in its composition and characteristics, but at the same time presents itself as one prominent secondary source of REE, makes this work more innovative and interesting in the current context. Therefore, it has the potential to drive emerging regulatory initiatives focusing on sustainable development and the circular economy, coupled with the increasing demand for strategic elements like REE, poised to surpass traditional research endeavors. These initiatives are likely to emphasize the exploration of low-cost treatment options and the identification of potential benefits associated with considering AMD as a viable secondary source.

Author Contributions: Conceptualization, G.C.S. and A.C.Q.L.; methodology, G.C.S. and L.P.T.N.; validation, C.S. and L.P.T.N.; formal analysis, A.C.Q.L.; investigation, G.C.S. and P.A.P.V.S.F.; resources, A.C.Q.L.; data curation, C.S.; writing—original draft, G.C.S., C.S. and A.C.Q.L.; writing—review & editing, C.S. and A.C.Q.L.; visualization, P.A.P.V.S.F.; supervision, A.C.Q.L.; project administration,

A.C.Q.L.; funding acquisition, A.C.Q.L. All authors have read and agreed to the published version of the manuscript.

Funding: This research was funded by MCTI, FAPEMIG, FINEP, CNPq, CAPES, the National Institute of Science and Technology for Mineral Resources Water and Biodiversity—ACQUA-INCT, Based Mineral High-Performance Materials and Processes Network—RENOVAMin (Proc. RED-00102–16) and Rare Earth Global Industry New Applications (REGINA) project.

Data Availability Statement: The original contributions presented in the study are included in the article, further inquiries can be directed to the corresponding authors.

Conflicts of Interest: The authors declare no conflict of interest.

References

1. Abrão, A. *Química e Tecnologia das Terras Raras*; CETEM/CNPq: Rio de Janeiro, Brazil, 1994.
2. Gupta, C.K.; Krishnamurthy, N. Extractive metallurgy of rare earths. *Int. Mater. Rev.* **1992**, *37*, 197–248. [\[CrossRef\]](#)
3. Balaram, V. Rare Earth Elements: A Review of Applications, Occurrence, Exploration, Analysis, Recycling, and Environmental Impact. *Geosci. Front.* **2019**, *10*, 1285–1303. [\[CrossRef\]](#)
4. Costis, S.; Mueller, K.K.; Coudert, L.; Neculita, C.M.; Reynier, N.; Blais, J.-F. Recovery potential of rare earth elements from mining and industrial residues case studies. *J. Geochem. Explor.* **2021**, *221*, 106699. [\[CrossRef\]](#)
5. Binnemans, K.; Jones, P.T.; Blanpain, B.; Van Gerven, T.; Pontikes, Y. Towards zero-waste valorisation of rare-earth-containing industrial process residues: A critical review. *J. Clean. Prod.* **2015**, *99*, 17–38. [\[CrossRef\]](#)
6. Hermassi, M.; Granados, M.; Valderrama, C.; Ayora, C.; Cortina, J.L. Recovery of rare earth elements from acidic mine waters: An unknown secondary resource. *Sci. Tot. Environ.* **2022**, *810*, 152258. [\[CrossRef\]](#) [\[PubMed\]](#)
7. Hermassi, M.; Granados, M.; Valderrama, C.; Skoglund, N.; Ayora, C.; Cortina, J.L. Impact of functional group types in ion exchange resins on rare earth element recovery from treated acid mine waters. *J. Clean. Prod.* **2022**, *379*, 134742. [\[CrossRef\]](#)
8. Simate, G.S.; Ndlovu, S. Acid mine drainage: Challenges and opportunities. *J. Environ. Chem. Eng.* **2014**, *2*, 1785–1803. [\[CrossRef\]](#)
9. Vaziri Hassas, B.; Shekarian, Y.; Rezaee, M. Selective precipitation of rare earth and critical elements from acid mine drainage—Part I: Kinetics and thermodynamics of staged precipitation process. *Resour. Conserv. Recycl.* **2023**, *188*, 106654. [\[CrossRef\]](#)
10. Larochelle, T.; Noble, A.; Ziemkiewicz, P.; Hoffman, D.; Constant, J. A Fundamental Economic Assessment of Recovering Rare Earth Elements and Critical Minerals from Acid Mine Drainage Using a Network Sourcing Strategy. *Minerals* **2021**, *11*, 1298. [\[CrossRef\]](#)
11. Van Gosen, B.S.; Verplanck, P.L.; Seal, R.R.; Long, K.R.; Gambogi, J. Rare-earth elements. In *Chapter O of Critical Mineral Resources of the United States—Economic and Environmental Geology and Prospects for Future Supply*; Schulz, K.J., DeYoung, J.H., Jr., Seal, R.R., Bradley, D.C., Eds.; U.S. Geological Survey: Reston, VA, USA, 1802; Volume 2017, pp. 1–31. [\[CrossRef\]](#)
12. Mwewa, B.; Tadie, M.; Ndlovu, S.; Simate, G.S.; Matinde, E. Recovery of rare earth elements from acid mine drainage: A review of the extraction methods. *J. Environ. Chem. Eng.* **2022**, *10*, 107704. [\[CrossRef\]](#)
13. Opare, E.O.; Struhs, E.; Mirkouei, A. A comparative state-of-technology review and future directions for rare earth element separation. *Renew. Sust. Energ. Rev.* **2021**, *143*, 110917. [\[CrossRef\]](#)
14. Nóbrega, A.F.; Lima, H.M.; Leite, A.L. Análise de múltiplas variáveis no fechamento de mina: Estudo de caso da pilha de estéril BF-4, Mina Osamu Utsumi, INB Caldas, Minas Gerais. *Rem Rev. Esc. Minas* **2008**, *61*, 197–202. [\[CrossRef\]](#)
15. Fernandes, H.M.; Franklin, M.R.; Veiga, L.H. Acid rock drainage and radiological environmental impacts. A study case of the Uranium mining and milling facilities at Pocos de Caldas. *Waste Manag.* **1998**, *18*, 169–181. [\[CrossRef\]](#)
16. Ouardi, Y.E.; Virolainen, S.; Mouele, E.S.M.; Laatikainen, M.; Repo, E.; Laatikainen, K. The recent progress of ion exchange for the separation of rare earths from secondary resources—A review. *Hydrometallurgy* **2023**, *218*, 106047. [\[CrossRef\]](#)
17. Hubicki, Z.; Koodynsk, D. Selective Removal of Heavy Metal Ions from Waters and Waste Waters Using Ion Exchange Methods. In *Ion Exchange Technologies*; InTech: London, UK, 2012; Chapter 8.
18. Abrão, A. *Operações de Troca Iônica*; IPEN/USP: São Paulo, Brazil, 2014.
19. Felipe, E.C.B.; Batista, K.A.; Ladeira, A.C.Q. Recovery of rare earth elements from acid mine drainage by ion exchange. *Environ. Technol.* **2020**, *1*, 2721–2732. [\[CrossRef\]](#) [\[PubMed\]](#)
20. Silva, G.C.; Bertoli, A.C.; Duarte, H.A.; Ladeira, A.C.Q. Recovery of rare earth elements from sulfate-rich acid mine water: Looking through the keyhole the exchange reaction for cationic resin. *J. Environ. Chem. Eng.* **2022**, *10*, 108715. [\[CrossRef\]](#)
21. Fernández, R.G.; Alonso, J.I.G. Separation of rare earth elements by anion-exchange chromatography using ethylenediaminetetraacetic acid as mobile phase. *J. Chromatogr. A* **2008**, *1180*, 59–65. [\[CrossRef\]](#)
22. Moore, B.W. Selective Separation of Rare Earth Elements by Ion Exchange in an Iminodiacetic Resin. U.S. Patent No. 6093376, 25 July 2000.
23. Moore, B.W.; Froisland, L.J.; Petersen, A.E. Rapid separation of heavy rare-earth elements. In *Report of Investigations*; Bureau of Mines: Washington, DC, USA, 1995.
24. Lindstrom, R.E.; Winget, J.O. Process for Separating Rare-Earth Elements by Ion Exchange. U.S. Patent No. 3228750, 11 January 1966.

25. Ding, Y.; David, H.; Wang, N.-H.L. Two-zone ligand-assisted displacement chromatography for producing high-purity praseodymium, neodymium, and dysprosium with high yield and high productivity from crude mixtures derived from waste magnets. *Green Chem.* **2020**, *22*, 3769–3783. [[CrossRef](#)]
26. José, L.B.; Ladeira, A.C.Q. Recovery and separation of rare earth elements from an acid mine drainage-like solution using a strong acid resin. *J. Water Process Eng.* **2021**, *41*, 102052. [[CrossRef](#)]
27. José, L.B.; Silva, G.C.; Ladeira, A.C.Q. Evaluation of Chelating Resins Efficiency in Recovering Rare Earth Elements from Sulphate-Rich Acid Solutions. *Environ. Prot. Res.* **2023**, *3*, 78–91. [[CrossRef](#)]
28. José, L.B.; Silva, G.C.; Ladeira, A.C.Q. Pre-concentration and partial fractionation of rare earth elements by ion exchange. *Miner. Eng.* **2024**, *205*, 108477. [[CrossRef](#)]
29. Thisani, S.K.; Von Kallon, D.V.; Byrne, P. Geochemical Classification of Global Mine Water Drainage. *Sustain* **2020**, *12*, 10244. [[CrossRef](#)]
30. Waber, N.; Schorscher, H.D.; Peters, T. Hydrothermal and supergene uranium mineralization at the Osamu Utsumi mine, Poços de Caldas, Minas Gerais, Brazil. *J. Geochem. Explor.* **1992**, *45*, 53–112. [[CrossRef](#)]
31. Wood, S.A. The aqueous geochemistry of the rare-earth elements and yttrium. 1. Review of available low-temperature data for inorganic complexes and the inorganic REE speciation of natural waters. *Chem. Geo.* **1990**, *82*, 159–186. [[CrossRef](#)]
32. Spahiu, K.; Bruno, J. *A Selected Thermodynamic Database for REE to Be Used in HLNW Performance Assessment Exercises*; MBT Tecnologia Ambiental: Cerdanyola, Spain, 1995.
33. Skoog, D.A.; West, D.M.; Holler, F.J.; Crouch, S.R. *Fundamentals of Analytical Chemistry*, 9th ed.; Brooks/Cole; Cengage Learning: Belmont, CA, 2014; 412p.
34. Dean, J.A. *Lange's Handbook of Chemistry*, 15th ed; MacGraw Hill: New York, NY, USA, 1999.
35. Pettit, L.; Powell, K. *IUPAC Stability Constants Database (SC-Database) Academic Software Data Version*; Academic Software: Otley, UK, 2005.
36. Melo, F.M.; Almeida, S.M.; Toma, H.E. Magnetic Nanohydrometallurgy Applied to Lanthanide Separation. *Minerals* **2020**, *10*, 530. [[CrossRef](#)]

Disclaimer/Publisher's Note: The statements, opinions and data contained in all publications are solely those of the individual author(s) and contributor(s) and not of MDPI and/or the editor(s). MDPI and/or the editor(s) disclaim responsibility for any injury to people or property resulting from any ideas, methods, instructions or products referred to in the content.